Wind Speed Discontinuity Related to Beaufort Wind Observations and Its Influences on Latent Heat Flux

Zhongxiang Wu
Department of Earth, Atmosphere, and Planetary Sciences
Massachusetts Institute of Technology

Kerang Li
Institute of Geography
Chinese Academy of Sciences

Introduction

The global oceans are the main energy source for our climate system. The oceans can absorb 65PW of direct solar radiation and 108PW of downward thermal radiation, two times more than the total absorbed by the atmosphere and land surfaces (Wood, 1984). The oceans redistribute the received energy through oceanic currents, and finally hand it over to the atmosphere in the forms of latent heat and sensible heat. The global oceans are more important than the continents in the hydrological cycle in the climate system. The oceans contribute 87% to the total world water budget which is about 577,000 km^3/yr, while the continents only 13% (Korzoun et al., 1977). Proper estimates of the energy fluxes and water vapor entering the atmosphere from the oceans are essential for modeling the climate and its variations. Great efforts have been made for quite a long time to achieve such estimates (e.g., Budyko, 1963; Esbensen and Kushnir, 1981; Hsiung, 1986), but the problems still exist. One example is given in Fig. 1 which is the time series of latent heat anomalies calculated using the COADS (Woodruff et al., 1987) for four tropical regions for the period of 1949-1990. The statistics and the significance test are given in Table 1. The positive trends obtained using the least square method are indicated by the dashed lines in the figure, and range from 17 Wm^{-2} in the eastern tropical Pacific (ETP) to 31 in Wm^{-2} the western tropical Pacific (WTP) during the 42-year period, all above the 95% significance level. Are these trends a real signal of climate change? The following discussion about the inhomogeneous wind observations and their influence on the latent heat flux may give us some clue to the answer.

Discontinuity of the Wind Observation

Some Japanese whaling ship data, which covered some data-sparse areas close to Antarctic region in COADS, were processed recently. The wind speed was recorded in Beaufort scale, providing therefore a relative uniform data set from one country using one method. The whaling ships usually passed the Australian coast and went to the area south of

50°S in the South Pacific before 1961, but afterward went through South China sea and entered the southern Indian Ocean during 1962-66. An example of ship track is shown in Fig. 2a. The wind measured by whaling ship from 1949 to 1961 in the region 50°–80°S, 120°E–80°W is plotted in Fig. 2b; the COADS wind is shown in Fig. 2c for the same region. During this period the whaling ships went to South Pacific. It is also during this period that the COADS winds all over the global oceans showed large positive trends (Wu and Newell, 1992). The dashed lines in Fig. 2b are the trends obtained by least square method. It is obvious that the wind trend in the whaling ship data is much smaller (0.16 ms^{-1}/13yrs) than that in COADS (2-26 ms^{-1}/13yrs).

The wind trend in COADS has been noticed by many researchers (e.g., Ramage, 1987; Cardone et al., 1990; Isemer and Hasse, 1991). Two factors were suggested to be the main contributors to the trend. One is the transfer of Beaufort wind observation to anemometer measurement, and the other the change of the ship size. Correcting the spurious trend needs much more work than locating its sources. Quantitative correction is needed, but is extremely difficult to get. It is almost unrealistic to correct the wind speed based on individual ships. It is not easy to find ships which conducted both scale wind observations and anemometer measurements to get hard numbers for the correction. The ship observations were usually not made in the same time and environment as that on nearby islands or buoys, which makes their intercomparison difficult considering the fact that the wind is the most variable component in the climate system.

Some land station data, however, may provide useful information for such correction. Most Chinese weather stations recorded the wind speed in Beaufort scale based on an instrument called wind-pressure plate, or on the states of smoke, dust, flag, trees etc., when wind-pressure plate was not available before late 1960s; and early 1970s. The instrument was very similar to the wind-force indicator in Hook's instruments, which was invented by Wild in about 1861 and used first by the British Royal Society (Khrgian, 1959). The Beaufort scale number on the wind-pressure plate was calibrated in wind tunnel according to WMO code 1100. The instrument was replaced by the standard cup anemometer around 1970. Most Chinese stations were established in early 1950s. There are 15-20 years of Beaufort wind observations and 20-25 years of anemometer measurements, which could be very useful to derive the quantitative correction needed in the COADS wind data. The cup anemometer was mounted at the same place as for the wind-pressure plate. The environment and observation schedule were also same as before. The systematic differences of the wind speed before and after were not likely caused by the natural variations. The way to get Beaufort scale number on the ship is different from that at Chinese land station, but both methods were calibrated by the WMO code 1100. They should reflect each other.

Parallel comparison of the wind speed measured by standard cup anemometer with that from wind-pressure plate has been done in many Chinese stations in the process of transfer. Unfortunately the data were not well collected and not too many survived. Table 2 is such comparison at 7 stations conducted at the time of the instrument changes. The wind-pressure plate was replaced by anemometer around the end of 1971. Column 2 is the wind speed converted using WMO 1100 from Beaufort scale obtained by wind-pressure plate, and column 3 the wind speed measured by cup anemometer simultaneously. The wind speed in these stations ranged from 4 to 12 ms^{-1}, corresponding to the Beaufort scale 4 to 6. The anemometer wind speed exceeded Beaufort wind speed at all stations, 17% on average. At Tomaho station, the anemometer wind speed was 27% higher than the Beaufort wind speed, but only 1% at Zanjan station. The ratio increased with the height of station.

The annual mean wind speed also showed similar changes. Table 3 gives the yearly averaged wind speed for 10 stations. The times of replacement of wind-pressure plate are shown by the underlined numbers. The wind speed increased at 8 stations after the replacement. The first five stations were located at high altitude, and all showed higher wind speed after the replacement. The other five stations were at low altitude near coast; three of them with weak wind speed showed 7-17% increase, but the two with relative strong wind speed showed 3-9% decrease. The t-test showed that the increases at four stations are above 95% significance level.

At high wind speed, however, the relationship is reversed. Table 4 is also the parallel comparison at 3 stations, but for strong wind (wind speed > 16ms^{-1}). The anemometer wind speed was much lower than Beaufort wind speed. The difference increased with the increasing of wind speed. It reached 10 ms^{-1} or more at Beaufort wind speed 34 ms^{-1}. The drop of the number of strong-wind days (wind speed > 16ms^{-1}) also reflected such tendency (Table 5). After the change from Beaufort wind observation to anemometer measurement, the number of strong-wind days were 16-90% less than before except at station Tia which showed only 1% decrease. At station Ron, the average of strong wind days was 27 days during the 7-year period before, but dropped to 3 days during the 11-year period after 1968 when the Beaufort wind observation was abandoned. Statistics showed that the changes at 4 stations are above 95% significance level.

Being consistent with the results of the Commission for Maritime Meteorology WMO in 1960 (CMM-IV, WMO, 1970), the above land observation data also show the feature that the Beaufort wind observations underestimate wind speed in low wind cases and overestimate wind speed in the strong wind cases. However, there are two points which deserve attention: one is that the difference between the Beaufort wind observation and the anemometer measurement increased with height, and the other is that the underestimate of strong wind was much larger than what CMM-IV showed.

The first point is related to the air density. Beaufort wind observation is based on the wind force F exerted on some object, which equals to:

$$F = c\rho s v^2 \qquad (1)$$

where ρ is the density of air, s the area of the subject perpendicular to the wind direction, v the wind speed and c the proportional coefficient. Density ρ is a function of temperature, pressure and water vapor, and could be 15% higher over the oceans in high latitudes than that over the tropical warm ocean areas, corresponding to a wind difference of 7% with higher wind speed in tropical, regions. The Beaufort scale equivalent wind of WMO 1100 was originally determined by the observations on the British island of St. Mary's (Scilly) which is located near 50°N. This equivalent wind scale would underestimate the wind speed in the warm, moist regions and overestimate in the cold, dry regions. Lin and Le (1975) deduced a correction coefficient, r,

$$r = 1.622\sqrt{T/(P - 0.378e)} \qquad (2)$$

where T, P and e are temperature, pressure and water vapor pressure respectively, to determine the anemometer wind speed corresponding to the Beaufort wind speed based on WMO 1100

in various conditions. This coefficient is listed along with the observed ratio between two wind speeds in the column 5 and 4 in table 2. They fit each other closely.

As to the second point, it is probably related the observation error of gusty wind. This is schematically shown in Fig. 3. Strong wind is always gusty, but the calibration of wind pressure plate is conducted in steady flow. The wind force F_2 exerts a torque on plate to balance the torque caused by F_1, which is related to the gravity force mg. The torque of wind is:

$$\tau = 0.5c\rho v^2 l^2 cos^2\alpha \qquad (3)$$

where ρ, l, and α are the line-density, the length and the angle of the plate. Assuming that the plate would be in position A at steady wind v_o, say 20 ms^{-1}, and that the wind is gusty and suddenly increases to this speed from v', say 17 ms^{-1}, when the plate is at position B with angle $\beta(<\alpha)$, the wind force and its torque exerted on the plate would be larger than that needed for the plate to stay at position A, and the plate would reach the position higher than A. The excess of the gusty wind torque is inversely proportional to the initial wind speed *v'*, and could be expressed in the form

$$\Delta\tau = cos^2\beta / cos^2\alpha_o \qquad (4)$$

where α_o is the calibrated angle for wind speed V_o. β can be determined by v' using

$$\sin\beta = \left\{-\lambda/v'^2 + \sqrt{(\lambda/v'^2)}\right)^2 + 4\}/2 \qquad (5)$$

$$\lambda = v_\circ^2 cos^2\alpha_\circ / sin^2\alpha_\circ \qquad (6)$$

Table 6 listed a sample calculation for v_o=20ms^{-1} and α_o=45°. It shows that a 20 to 30% overestimate of torque in gusty winds is quite possible by Beaufort wind observation.

This principle should work to the surface wind waves in the ocean. The wind energy transmitted to the surface wind wave can be expressed in the form (Titov, 1969)

$$N_w = Ah(w-c)^2 \qquad (7)$$

where A is a constant, h the wave height, w the wind speed and c the wind wave speed. This form is similar to (1). The gusty wind could give the observer an impression of higher Beaufort scale. But the magnitude of the overestimate would be much smaller because of the large inertia of the surface wave. This could be one of the reasons for the overestimate of wind speed at high Beaufort scales.

Influence of the wind trend on the latent heat flux

Wind is the major factor controlling the evaporation at ocean surface. The wind trend was shown globally (Wu and Newell, 1992), and needed to be considered in the calculations of latent heat flux. The wind speed obtained by Beaufort wind observation was transferred back to its Beaufort scale using WMO 1100, then transferred to CMM-IV equivalence, a better code than WMO 1100 (WMO, 1970). Since most ships were higher than 10 meters, the height required by bulk equation, the anemometer wind speed was subjected evaporation to the height adjustment using the equations (Smith, 1980; Wu, 1980)

$$\frac{U_z}{u_*} = \frac{1}{\kappa} \ln \frac{z}{z_\circ} \tag{8}$$

$$\frac{z_\circ}{\frac{u_*^2}{g}} = a \tag{9}$$

Where U_z is the wind speed in height z, u_* the friction velocity, κ the von Karman constant and z_o the roughness length. The a in (9) is a constant and equals 0.00185. The ship height has assumed to be 20 meters (Cardone et al., 1990). The Newton iterative method was used along with the measured wind to find z_o, then calculate the wind speed at 10 meters. The ratio of Beaufort wind observations to anemometer measurements from Ramage (1987).

The latent heat flux was calculated using bulk equation except in the light wind condition over warm ocean surface where the Stelling formula was used (Brutsaert, 1982). the transfer coefficient from Large and Pond (1982) was used form neutral conditions, and adjusted for other conditions following the ratios of Isemer and Hasse (1991).

The evaporation in light wind over warm pool region needs to be considered with extra caution. The bulk equation is base on the formula of evaporation

$$E_z = -\rho k_z \frac{\partial q}{\partial z} \tag{10}$$

where E_z is the water vapor flux in the z-direction and $\partial q/\partial z$ the vertical gradient of the specific humidity. k_z, is the eddy diffusivity for water vapor, and is determined by the vertical wind profile on the proposition that the eddy diffusivity for the water vapor is the same as that for momentum. Assuming the vertical wind profile near the surface follows the logarithmic distribution, the above formula can be expressed in the form

$$E_z = -\rho c_e (u_2 - u_1)(q_2 - q_1) \tag{11}$$

$$c_e = \frac{\kappa_2}{\ln \frac{z_2 + z_0}{z_1 + z_0}} \tag{12}$$

where κ is the von Karman's constant. The bulk equation is the specific case of this form when u_1 equals zero. The vertical transport of water vapor related to buoyancy is not included in the bulk equation, and therefore there would be no evaporation if there is no wind. In the warm pool region, where the wind speed is the lowest and the surface temperature the highest over the global ocean, the buoyancy effect should not be neglected.

The latent heat fluxes measured in the tropical west Pacific at zero wind speed is 25 Wm^{-2} (Bradley et al., 1991). Newell et al. (1978) and Newell (1979, 1986) proposed that net heat flux should be close to zero when the SST reaches its limit of 30°C because of the buffering of the evaporation. Using the experiment data measured from the ship R/V Franklin, Godfrey and Ländstrom (1989) have shown that the net heat flux is near zero at the sea surface near New Guinea. The ocean mixing and advection processes in the western equatorial Pacific are too weak to carry away heat flux more than 10 Wm^{-2}. The current results are from 20 to 100 Wm^{-2} (Esbensen and Kushnir, 1981; Reed, 1985). A fine adjustment of latent heat in low wind speed over the tropical ocean surface does matter to the ECMWF model forecast (Miller et al., 1992). A new parameterization of evaporation, which raises the latent heat flux from zero to about 25 Wm^{-2} at calm weather condition, can greatly improve the model simulation, including the rainfall distribution, monsoon circulation et al.

Stelling first formulated an equation in 1882 to include the zero wind evaporation (Brutsaert, 1982)

$$E = A_s + B_s u\left(e_s^* - e_a\right) \tag{13}$$

where A_s = 0.0702 and B_s = 0.00319. E is the evaporation in mm/(2 hrs), u the wind speed in km/hr at 7.5 in above the surface, and e the water vapor pressure in min Hg. This formula is still widely used in engineering with various coefficients of A_s and B_s.

Stelling formula was used to calculate the latent heat flux in the light wind ($u < 3 ms^{-1}$) and warm SST (≥ 28.5°C) conditions. But the coefficients need to be determined since the original ones were only suitable for the continent region at high latitude. The averaged values of q_s - q_a and T_s - T_a in the light wind and warm SST circumstances are 6.75 g/kg and 2.23°C according to the COADS. Assuming that the bulk equation is valid for the wind speed of 3 ms^{-1} and above, and that the latent heat flux is 25 Wm^{-2} at zero wind speed, the Stelling equation would be

$$Q_L = 3.70 + 3.952u)(q_s - q_a) \tag{14}$$

where Q_L is latent heat flux in Wm^{-2}, u and q are in ms^{-1} and g/kg, respectively.

The time series of latent heat flux and their trends for the same regions in Fig. 1 are shown in Fig. 4, and their statistics included in Table 1. The trends are greatly reduced, very close to zero in the ETP and tropical Atlantic. They are about 10 Wm^{-2} in the WTP and the western tropical Indian ocean, but the estimated errors of the coefficient b for trends are overlapped with zero at 95% significance level and therefore the remained trends may not be real.

The effect of wind adjustment on the climatology of latent heat flux is shown in Fig. 5, which is the differences between latent heat fluxes calculated with and without wind adjustment for January, July and yearly mean. The adjustment raises the latent heat fluxes about 5-10 Wm^{-2} over the tropical and subtropical oceans, but lowers the fluxes about 5 Wm^{-2} over the oceans in the middle and high latitudes. Comparing with the wind climatology, it is found that the zero line corresponds to the wind speed of 8 ms^{-1}, below which the latent heat correction is positive and vice versa. Generally speaking, however, the adjustment does not change the pattern of the latent heat flux.

It seems impossible to justify the individual wind correction in COADS, but there are some constraints which could be used to test the validity of adjustment as a whole. One constraint is the water balance. The difference of the evaporation and the precipitation (*E*-*P*) over the global oceans should be balanced by the river runoff. It was calculated using the Q_L and Jaeger's predication (Jaeger, 1976). The results are listed in Table 7. The total water deficit of oceans is $47.2 \times 10^3 km^3 yr^{-1}$. The UNESCO (1978) river flow into three oceans is $41.7 \times 10^3 km^3 yr$ and underground flow $2.2 \times 10^3 km^3 yr^{-1}$. The water deficit obtained with unadjusted wind is $29.9 \times 10^3 km^3 yr$. The latent heat flux calculated using adjusted wind ends up with a better water balance coinciding the fact that the values of *E*–*P* south of 40°S are not all included because of missing data and that the precipitation there is usually larger than the evaporation.

Another constraint is the total net heat flux entering the oceans. Latent heat flux affects not only the water balance but also the energy balance of the oceans. The global mean net heat flux of the oceans should be very close to zero since the oceanic temperature is quite stable on the time scale of several decades. The global averaged net heat flux of Esbensen and Kushnir (1981) is 5 Wm^{-2} and the lowest among others, which would warm the global oceans 0.1°C per decade, and Hsiung's and Weare's numbers would result in more warming (Reynolds, 1988). The net heat flux of Reed in the tropical Pacific is about 80 Wm^{-2} more than Esbensen and Kushnir's number and would lead to tremendous warming of the ocean. The global mean of net heat flux after taking account of wind correction is given in Table 8. The long term annual mean is 1 Wm^{-2}, close to zero, but the amplitude of seasonal variation could reach 30 Wm^{-2}. The oceans lose more heat in northern winter, which is the results of the strong latent heat and sensible heat losses in the Gulf Stream and Kuroshio regions.

The energy balance in the warm pool region is also a constraint. The net heat fluxes in this region should be close to zero (Newell et al., 1978; Newell, 1979, 1986; Godfrey and Ländstrom, 1989). The time series of the net heat fluxes in WTP and ETP regions are given in Fig. 6. The 12 -months running mean (dash line) is close to zero in the WEP region, but 40-50 Wm^{-2} in the ETP region except during the strong El Niño in 1982-83 period when the SSTs there were close to sea surface temperature limit (Newell, 1986).

Summary

Beaufort-only wind data from Japanese whaling ship did not show positive trend for the period of 1949 - 61 while the wind speed from COADS increased 2.26 ms^{-1} during this period. A homogeneous wind data set may give us a picture about trend closer to the reality than mixed data set. More efforts are needed to search for such data sets in order to verify our knowledge about the climate changes.

Parallel comparison of Beaufort wind observation with anemometer measurements at land stations confirms the fact that Beaufort scale wind could underestimate wind speed at low wind speed and overestimate wind speed at high wind speed. The comparison shows that difference between Beaufort wind and anemometer wind increases when the air density decreases. The bias of Beaufort scale wind would be more in warm and moist region than that in cold and dry region. The overestimate of Beaufort scale at high wind speed is more severe at land stations. The gusty nature of wind is the main source for the overestimate error. The same principle should work for the wind waves at ocean surface.

The wind trend in COADS causes spurious latent heat trend. According to this trend, the latent heat flux received by the atmosphere would be 30 Wm^{-2} more in 1990 than in 1949 in the WTP alone. If the COADS wind is adjusted following the CMM-IV code, and then used in the latent heat calculation, the latent heat trend is reduced significantly, failing to pass the statistic test in most regions. The global water balance, the energy balances of the global oceans and of the warm pool region support the wind adjustment, which leads to more reasonable results.

Acknowledgments

Z. Wu was supported by the National Science Foundation Climate Dynamics Program under Grant No. ATM 9106902. We thank S.M. Leite, a UROP student at MIT, for the Japanese whaling ship data input.

References

Bradley, E. F., P. A. Coppin and J. S. Godfrey, 1991: Measurements of Sensible and Latent Heat Flux in the Western Equatorial Pacific Ocean. *J. Geophys. Res*., 96, 3375-3398.

Brutsaert, W., 1982: *Evaporation into the Atmosphere*. D. Reidel Publishing Company, London, 299 pp.

Budyko, M.I., 1963: *Atlas of the Heat Balance of the Earth*. Gidrometeorozdat, Moscow, 69 pp.

Cardone, V.J, J.G. Greenwood and M. Cane, 1990: On Trends in the Historical Marine Wind Data. *J. of Climate*, 3 113-127.

Esbensen, S.K., and Y. Kushnir, 198 1: The Heat Budget of the Global Ocean: An Atlas Based on the Estimates from Surface Marine Observation. Rep. 29, 27 pp., Climatic Res. Inst. Oregon State Univ., Corvallis.

Godfrey, J. S. and E. J. Ländstrom, 1989: The Heat Budget of the Equatorial Western Pacific Surface Mixed Layer. *J. Geophys. Re*s., 94, 8007-8017.

Hsiung, J., 1986: Mean Surface Energy Fluxes over the Global Ocean. *J. Geophys. Res*. 91, 10585-10606.

Isemer, H.J. and L. Hasse, 1991: The Scientific Beaufort Equivalent Scale: Effects on the Wind Statistics and Climatological Air-Sea Flux Estimates in the North Atlantic Ocean. *J. of Climate*, 4, 819-836.

Jaeger, L., 1976: Monatskarten des Niederschlags für die ganze Erde. *Ber. Der Deutsche Wetterd*., 18 No. 13 9, 3 8 pp.

Khrgian, A.K., 1959: Meteorology, A Historical Survey. Vol. 1, 387 pp., GIMIZ, Gidrometeorologicheskoe Izdatel'stove, Leningrad.

Korzoun, V.I., A.A. Sokolov, M.I. Budyko, K.P. Voskrensky, G.P. Kalinin, A.A. Konoplyantsev, E.S. Korotkevich and M.I. Lvovich, 1977: *Atlas of World Water Balance*. UNESCO Press, Paris, 34 pp and 65 maps.

Large, W., and S. Pond, 1982: Sensible and latent Heat Flux Measurements over the Ocean. *J. Phys. Oceanogr*., 12, 464-482.

Lin, G. and Li K., 1975: Problems of Wind Speed Related to the Instrument Changes. Science and Technology in Meteorology (in Chinese), 3, 5-10.

Miller, M. J., A. C. M. Be1jaars and T. N. Palmer, 1992: The Sensitivity of the ECMWF Model to the Parameterization of Evaporation from the Tropical Oceans. *J. Climate*, 5,418-434.

Newell, R. E., A. R. Navato and J. Hsiung, 1978: Long-term Global Sea Surface Temperature Fluctuations and their Possible Influence on the Atmospheric C02 Concentrations. *Pure and Appl. Geophys*., 116: 3 51-3 7 1.

Newell, R. E., 1979, Climate and the Ocean. *American Scientist*, 67: 405-416.

Newell, R. E., 1986: El Niño: An Approach towards Equilibrium Temperature in the Tropical Eastern Pacific. *J. Phys. Oceanogr*., 16: 1338-1342.

Ramage, C.S., 1987: Secular Change in the Reported Surface Wind Speeds over the Ocean. *J. Climate and Appl. Meteor*., 26, 525-528.

Reed, R.K., 1985: An Estimate of the Climatological Heat Fluxes over the Tropical Pacific Ocean. *J. Clim. Appl. Meteor*., 24, 833-840.

Reynolds, R.W., 1988: Computation of the Global Air-Sea Flux Climatology. Atmospheric Forcing of Ocean Circulation, Tulane University, New Orleans, Louisiana p20-40.

Smith, S.D., 1980: Wind Stress and Flux over the Ocean in the Gale Force Wind. *J. Phys. Oceanogr*., 10, 709-728.

Woodruff, S.D, R.L. Slutz, R.L. Jenne and P.M. Steurer, 1987: A comprehensive Ocean Atmosphere Data Set. *Bull. Amer. Meteor. Soc*. 68, 1239-1250.

Woods, J.D., 1984: The Upper Ocean and Air-Sea Interaction in Global Climate. 141-181, in *The Global Climate*. J.T. Houghton (Ed.), Cambridge University Press, Cambridge, 233 pp.

Titov, L.F., 1969: Wind -Driven Waves. p78, translated from Russian, Israel Program for Scientific Translations Ltd., Keter Press, Jerusalem.

UNESCO, 1978: World Water Balance and Water Resources of the Earth. *Unesco Series Studies and Reports in Hydrology*, 25, Leningrad, 663pp.

WMO, 1970: The Beaufort Scale of the Wind Force. Report No. 3, Geneva, Switzerland, pp. 22.

Wu, J., 1980: Wind Stress Coefficients over Sea Surface near Neutral Conditions - a Revisit. *J. Phys. Oceanogr*., 10, 727-740.

Wu, Z and R.E. Newell, 1992: The Wind Problem in COADS and Its Influence on the Water Balance. In H. F. Diaz, K. Wolter and S. D. Woodruff (eds.) Proceedings of the International COADS Workshop, Boulder, Colorado, pp. 189-200.

Table 1: Trends of the latent heat fluxes in the tropical regions.

Region	Without Adjustment			With Adjustment		
	b	δb	trend (Wm^{-2})	b	δb	trend (Wm^{-2})
Trop W. Pac.	0.536	0.234	30.7(Y)	0.195	0.231	9.5(N)
Trop E. Pac.	0.354	0.214	16.6(Y)	-0.006	0.215	-0.2(N)
Trop. Atl.	0.569	0.139	19.7(Y)	0.050	0.140	1.4(N)
Trop. W. Ind.	0.492	0.238	27.6(Y)	0.208	0.230	10.0(N)

Note: b is the linear coefficient of the trend, and b its error. Y/N indicates above/below 95% significance level.
Coordinates of the regions are:

Trop. W. Pac: 10° S - 10°N, 140° E - 180°;
Trop. E. Pac: 10°S - 0, 120°W - 80°W;
Trop. Atl: 5°S - 10° N, 40°W - 10°:
Trop. W. Ind.: 5°S - 5°N, 40°E - 60°.

Table 2: Parallel comparison of Beaufort Wind Sped with anemometer wind speed.

stn.	Height(m)	W_b ms^{-1}	W_a ms^{-1}	W_a/W_b (obs)	W_a/W_b (cal)	obs.	month/year
Tomaho	4700	9.60	12.16	1.27	1.278	35	12/1971
Wudolan	4700	8.29	10.24	1.26	1.27	32	12/1971
Mado	4222	7.58	9.10	1.20	1.23	52	12/1971
Goulo	3719	7.56	8.87	1.16	1.21	32	12/1971
Zaka	3086	6.81	8.23	1.21	1.18	22	11/1971
Daton	2567	5.16	5.65	1.10	1.12	20	11/1971
ZanJan	26	4.60	4.66	1.01	1.00	5	1/1972

Table 3: Annual Mean wind speeds before and after replacement of wind pressure palate at 10 stations.

yr	Chu	Jin	Bal	Ban	Min	Tia	Wen	Don	Chi	Bin
60	-	-	-	-	-	2.9	4.7	7.2	3.9	7.6
61	2.1	2.5	3.6	3.2	1.9	2.8	4.2	7.3	4.2	7.8
62	-	2.6	2.6	2.9	2.2	3.0	4.7	7.0	3.5	7.3
63	2.5	2.4	2.6	2.5	2.2	2.9	4.0	6.4	3.4	6.3
64	2.7	2.4	2.9	3.1	1.8	2.6	3.8	8.0	3.3	7.4
65	2.6	2.2	2.6	2.8	1.6	2.8	4.4	7.4	3.4	6.9
66	2.8	2.3	2.7	3.2	1.8	2.7	4.5	7.1	3.8	6.4
67	2.4	2.2	3.0	3.1	1.4	2.7	3.7	7.4	3.6	6.5
68	2.9†	2.6	2.3	3.1	2.3	2.9	3.8	7.1	3.3	6.1
69	3.6	3.5	2.7	3.5	2.3	3.1	4.0	6.5	3.7	6.2
70	3.5	3.5	3.6	4.9	2.3	3.1	3.9	7.0	3.7	6.2
71	2.9	3.1	4.0	4.4	2.1	3.3	4.1	6.9	3.7	6.1
72	2.8	3.1	2.7	4.5	2.0	3.3	4.2	6.9	4.0	6.0
73	2.7	3.2	3.4	4.6	2.3	3.1	4.1	7.4	4.1	6.4
74	2.3	3.3	3.8	4.8	2.2	3.3	4.2	7.5	4.2	6.6
75	2.3	3.0	3.9	4.7	2.0	3.0	4.1	6.8	4.3	5.8
76	2.6	3.3	-	-	2.0	2.8	4.2	6.9	4.3	6.5
77	2.4	3.2	-	-	1.7	2.5	3.9	6.1	4.1	6.8
78	-	3.2	-	-	1.4	2.5	5.9	6.9	4.1	6.5
79	2.4	3.1	-	-	1.5	2.7	5.8	6.7	4.4	6.0
80	2.3	3.0	-	-	1.5	3.3	5.7	6.8	4.2	5.8
$\bar{v}_1$	2.6	2.4	2.7	3.0	1.87	2.8	4.2	7.1	3.6	6.9
$\bar{v}_2$	2.7	3.2	3.6	4.7	2.0	3.0	4.7	6.9	4.2	6.3
Δv(%)	4.0	33.0*	33.0*	57.0*	11.0	7.1	11.9	-2.8	16.7*	-8.7*

†: The corresponding year was the year of replacement of wind-pressure plate.
$\bar{v}_1$, $\bar{v}_2$: The mean annual wind speeds before and after the replacement.
*: above 95% significance level.

Table 4: Parallel comparison of maximum wind speeds from Beaufort scale and anemometer at 3 stations.

Station	W_b*(ms^{-1})	34.0	28.0	24.0	20.0	18.0	17.0
Kanemen	W_a†	22.9	18.9	18.7	16.8	15.3	15.4
	obs.	4	3	28	31	27	13
Sanbo	W_a	24.1	22.0	20.0	18.6	-	-
	obs.	2	4	8	4	-	-
Wanjan	W_a	23.5	21.2	19.2	17.5	16.1	15.1
	obs.	4	9	18	19	24	3
Average	W_a	23.5	21.0	19.1	17.2	15.7	15.4
	obs.	10	16	54	54	51	16

*: Beaufort wind speed; †: anemometer wind speed.

Table 5: The changes of number of strong wind days at 6 stations.

yr	Ron	Tia	Jia	Don	Chi	Bin
61	-	39	-	132	139	126
62	-	27	-	128	113	106
63	36	38	16	100	105	81
64	34	21	14	165	94	150
65	22	42	22	147	106	108
66	25	47	28	141	128	88
67	15	50	13	140	136	81
68	26	39	28	142	105	51
69	36†	32	30	113	83	60
70	5	32	16	105	58	53
71	4	23	12	95	50	80
72	1	44	17	100	55	53
73	0	32	8	133	84	83
74	1	39	17	125	57	106
75	1	37	14	104	73	58
76	0	34	16	111	76	67
77	0	43	12	82	75	101
78	2	57	17	96	85	94
79	4	43	-	91	107	72
80	14	34	-	122	76	108
$\overline{N}_1$	27.7	37.9	21.4	134.2	101.5	94.6
$\overline{N}_2$	2.7	37.5	14.3	105.8	76.4	79.5
ΔN(%)	-90.3*	-1.1	-33.2*	-21.2*	-24.7*	16.0

†: corresponding year was the year of replacement of wind-pressure plate.
$\overline{N}_1$: averaged strong wind days before replacement.
$\overline{N}_2$: averaged strong wind days after replacement.
*: above 95% significance level.

Table 6: Gusty wind effect on the torque of wind-pressure plate†

Initial wind speed (ms^{-1})	15.0	16.0	17.0	18.0	19.0	20.0
$\tau_{gust}/\tau_{steady}$	1.389	1.304	1.221	1.143	1.069	1.000

†: Assuming the calibrated position of the plate to be 45° at wind speed of $20ms^{-1}$.

Table 7: Water budget in three oceans (unit: 10^3 km^3).

	PAC			ATL			IND			ALL		
	N	S	N+S	N	S	N+S	N	S	N+S	N	S	N+S
P	112.2	115.9	228.1	48.4	31.3	79.9	18.6	62.4	81.0	179.2	209.6	388.8
E	115.1	96.8	211.9	61.8	37.7	99.5	19.5	62.6	81.7	196.3	196.7	393.1
E-P	3.4	2.3	5.7	14.8	12.2	27.0	0.9	13.7	14.6	19.1	28.2	47.2

Table 8: Monthly global mean of net heat flux (unit: W/m^2).

JAN	FEB	MAR	APR	MAY	JUN	JUL	AUG	SEP	OCT	NOV	DEC	YR
-9.3	1.0-	12.4	13.2	7.8	1.78	4.8	4.2	9.4	-0.82	-11.1	-15.2	1.0

Figure 1: The time series of latent heat flux without wind correction (solid lines) in four tropical oceanic areas. The dashed lines are the trends obtained by least square method.

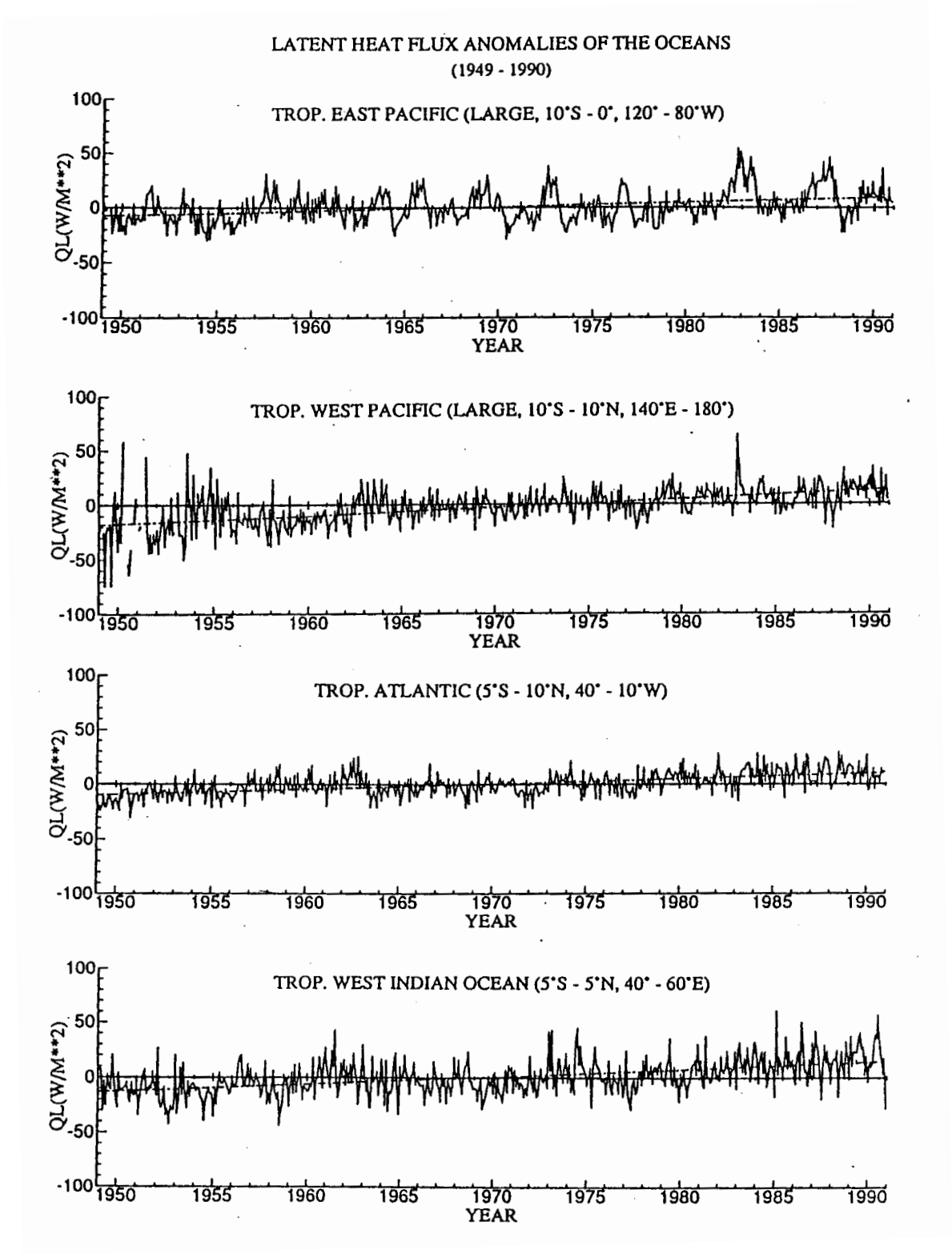

Figure 2: Japanese whaling ship route (top), measured wind (middle) and the COADS wind in the same region.

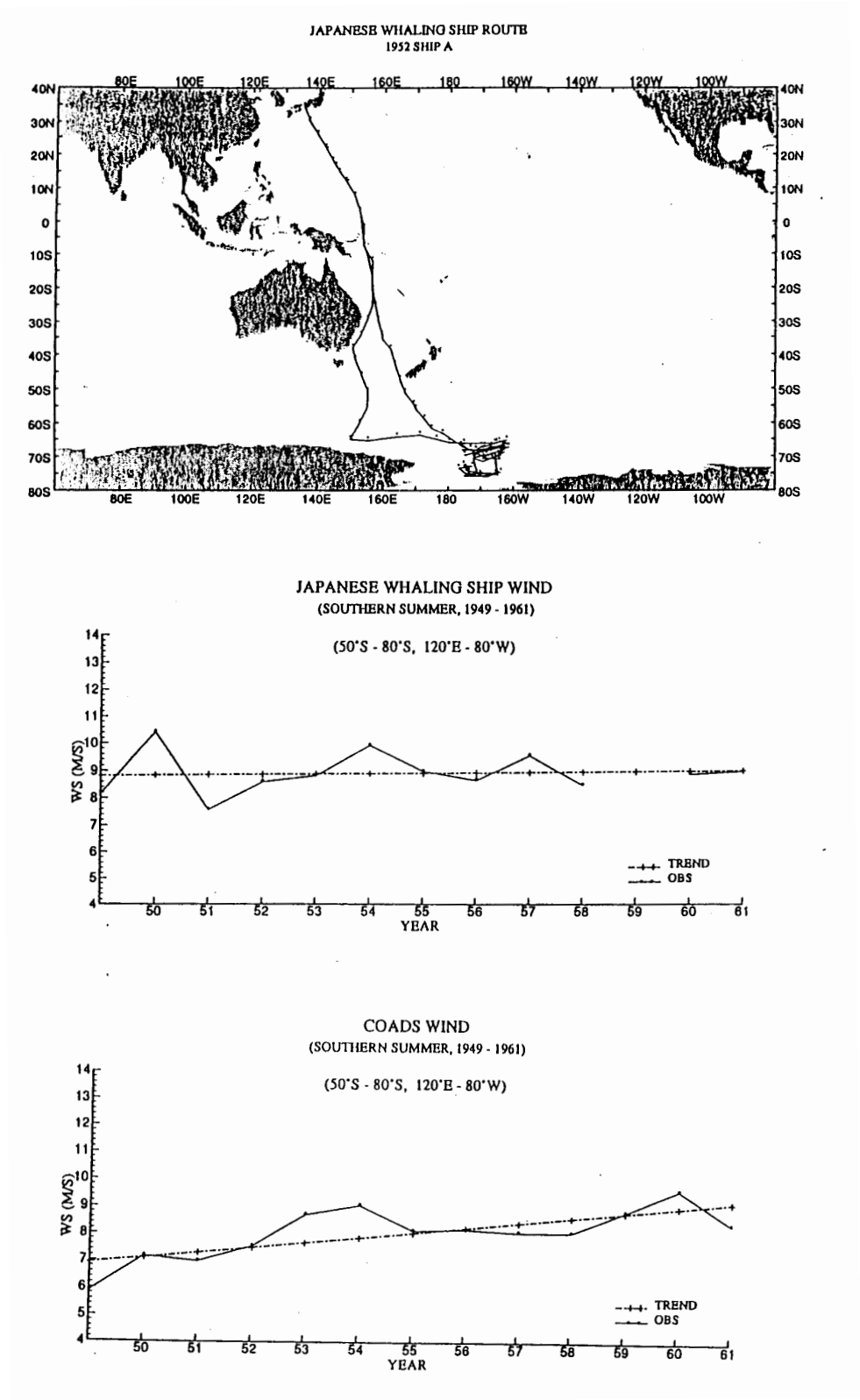

Figure 3: Forces exerted on the wind plate.

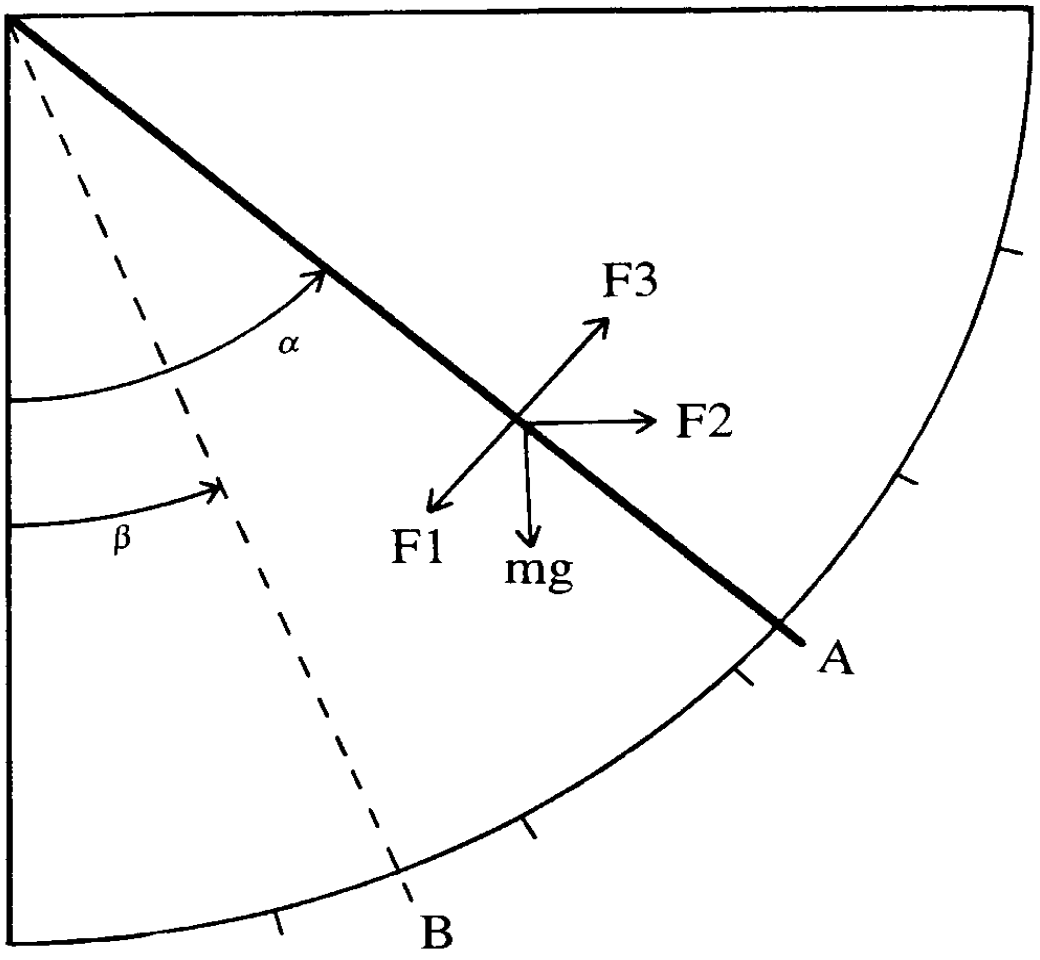

Figure 4: Same as Fig. 1 but with wind correction.

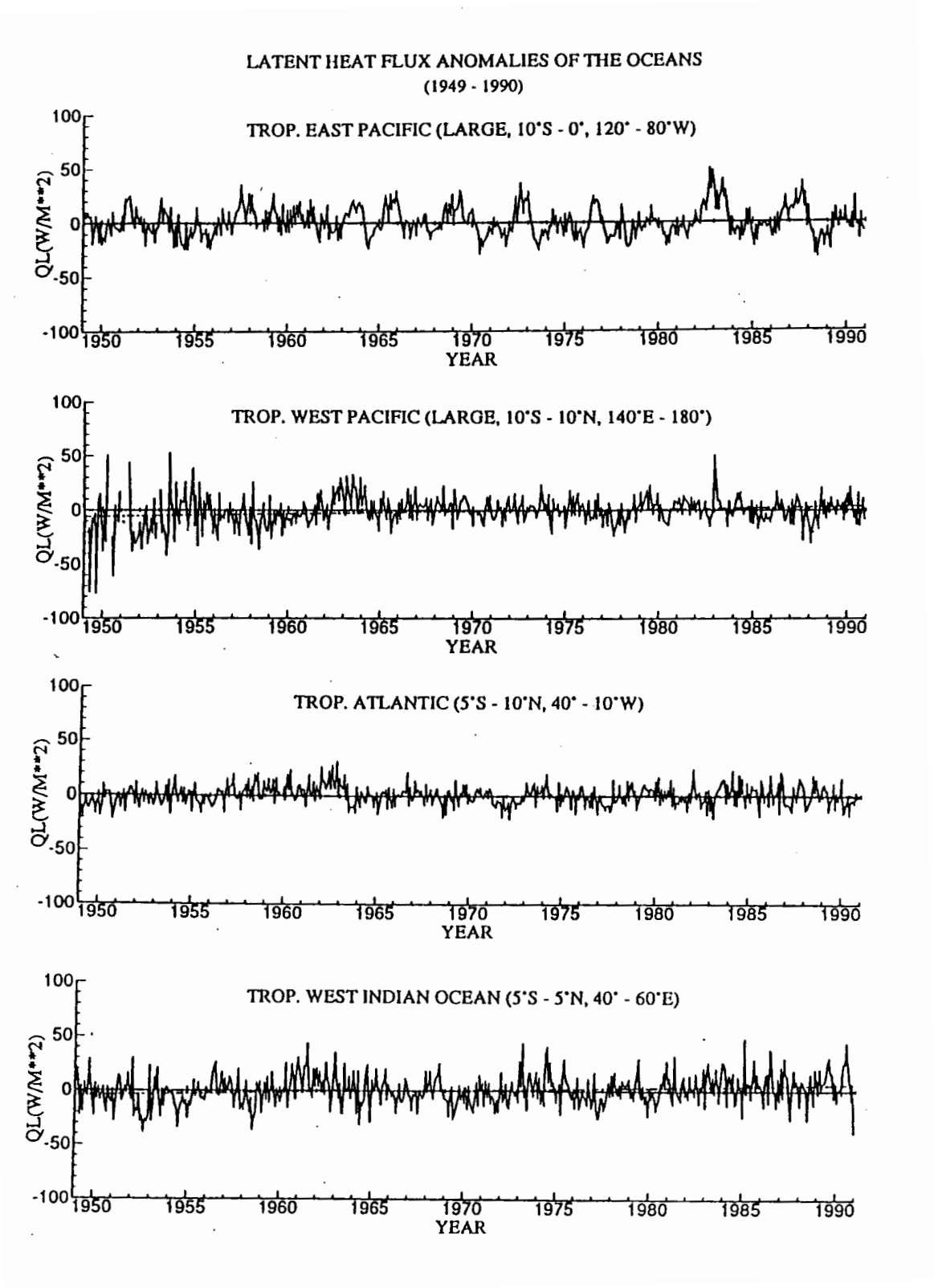

Figure 5: The effects of wind correction on the latent heat flux.

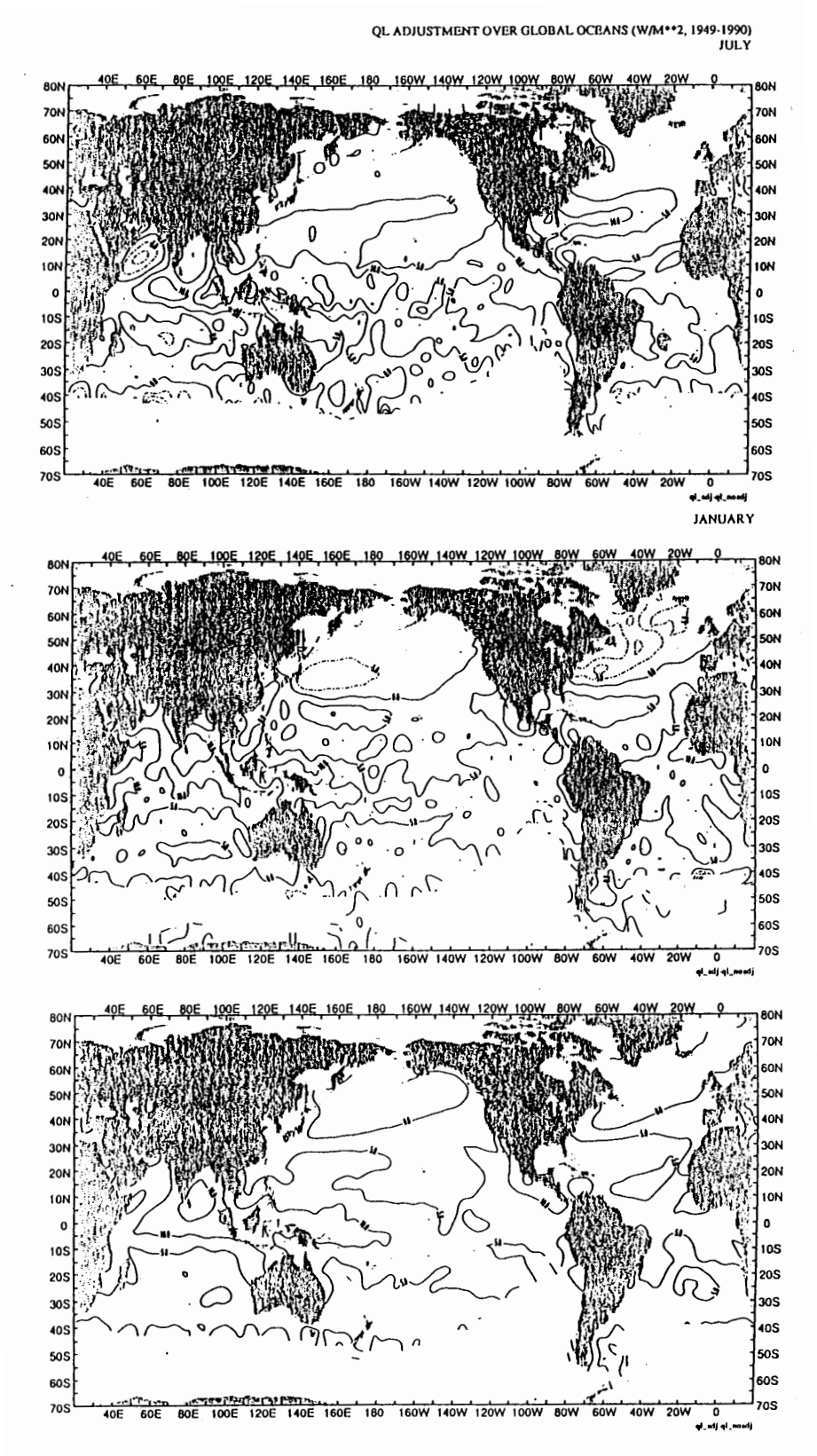

Figure 6: Net heat flux into the ocean in the western and eastern tropical Pacific Oceans.